THE MENAGERIE OF GEOSPACE PLASMA WAVES

Stanley D. Shawhan
Office of Space Science and Applications
NASA Headquarters Code EES
Washington DC 20546 USA

ABSTRACT. Sounding rockets and satellites have discovered a large variety of plasma waves within the Earth's magnetosphere--geospace. These waves are found over a frequency range of millihertz to megahertz. The frequency ranges are generally associated with characteristic frequencies such as the plasma frequency and gyrofrequency. Most waves are generated by hot or streaming magnetospheric plasma; some waves are due to lightning discharges, to intentional man-made transmitters or to incidental radiation from power transmission systems. Propagation of waves from the observation region back to a probable source region can be modelled using ray tracing techniques in a model magnetosphere where the electron number density, ion composition and magnetic field vector is specified. Information in addition to the common amplitude-frequency-time spectrograms can be obtained from the received waves using multiple antennas and receivers. Cross-correlation of the wave electric and magnetic components can provide information on the wave polarization and direction of propagation and on the wave distribution function.

1. INTRODUCTION

Geospace is considered the region surrounding the Earth out beyond the bow shock at 20 R_E on the dayside to more than 250 R_E on the nightside of the Earth. This region contains plasma above about 80 km altitude and plasma is the predominant state of matter above 250 km. Plasma waves have been found to occur throughout geospace through numerous sounding rocket and satellite measurements. The term plasma wave is meant to specify all waves which are generated in a plasma or interact with the plasma medium as they propagate through; space plasma waves are found in geospace, the interplanetary medium, at other planets and in the solar corona. See for example Scarf (1985) and Kimura (1985) in this volume.

Within geospace there is a menagerie of plasma waves types. Figure 1 identifies many of these types by commonly used names. In a given spatial region a number of types can occur simultanenously in

Space Science Reviews **42** (1985) 257–274. 0038–6308/85.15

several different frequency ranges. The total range observed covers millihertz to megahertz. Specific frequencies are dependent on frequencies characteristic of the plasma which generally decrease at greater distance from the Earth since they depend on plasma density which varies by six orders of magnitude and on magnetic field which varies by five orders of magnitude. Both electromagnetic and electrostatic waves can exist; both types can generally be described mathematically through plasma dispersion relations (Stix, 1962). Almost all of the plasma waves types can propagate from the source region to other remote regions, but cannot escape the plasma medium into free space. One type, the Auroral Kilometric Radiation (AKR), does escape to make the Earth a cosmic radio source at a power level of 1 billion watts.

Geospace waves are named for a variety of reasons: for the region in which they occur--such as auroral kilometric radiation and plasmaspheric hiss, for the way they sound when played through a speaker--such as whistlers and lion roars, or for the association with a characteristic frequency--such as the upper hybrid resonance frequency--UHR noise, for example. Naturally occurring plasma waves are found to be the result of electromagnetic energy from lightning discharges coupled into the magnetosphere or to energy transfer from hot or streaming plasma. Man-induced waves are also readily detected. These waves may be due to intentional transmitters such as very low frequency (VLF) code transmitters or to incidental radiation from high voltage power transmission lines. A compendium of wave types, observed frequency range, geospace location and observed characteristics is given in Table 1. Even more detailed reviews about specific wave types are given in works by Helliwell (1965), Al'pert (1974), Gendrin (1975), Shawhan (1979a) and Anderson (1983), for example. This tutorial paper draws heavily on these papers and a few other published works which are cited as appropriate. Each of these works contains an extensive bibliography which should be consulted for additional information.

The purpose of this tutorial paper is to provide some insight as to why geospace plasma waves occur in frequency and space as observed, to identify the types of sources for these waves, to describe a typical plasma wave receiving system and provide illustrations of wave types detected and displayed on spectrograms, to establish a basis for understanding the ray tracing procedure with sample results, to describe the type of information that can be obtained from analysis of multiple wave components including polarization, and up/down propagation and the wave distribution function, and to suggest areas needing further research.

2. CHARACTERISTIC FREQUENCIES AND SOURCE MECHANISMS

By assuming a plane wave solution to the wave equation for an infinite, homogeneous plasma with cold electrons and ions and a permeating magnetic field, a dispersion relation for electromagnetic plasma waves can be derived (Stix, 1962):

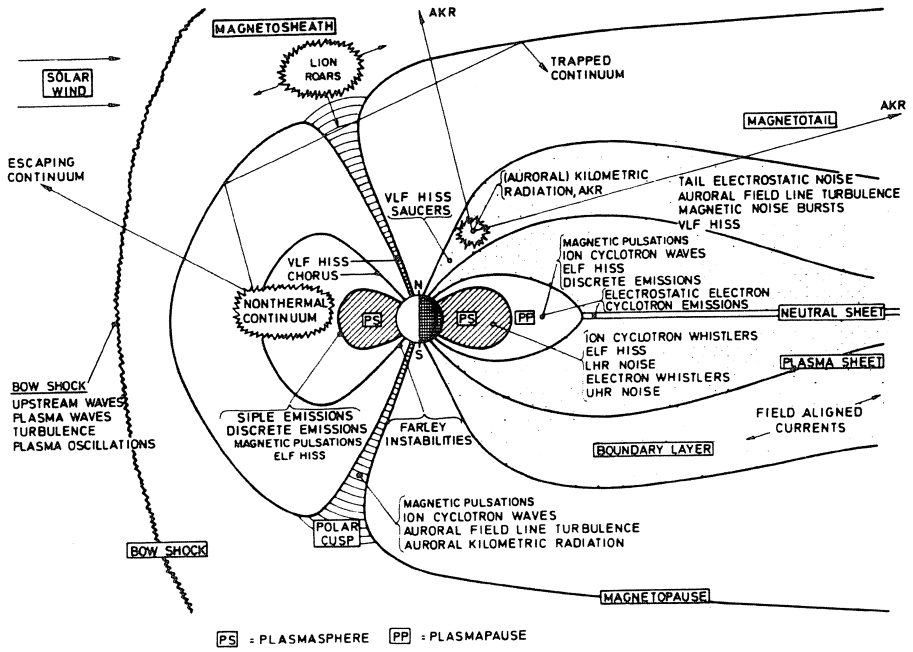

Figure 1. The menagerie of geospace plasma wave types located on a noon-midnight cross-section of the Earth's magnetosophere (Shawhan, 1979a).

$$n = ck/2\pi f \qquad (1)$$

where $\underline{k}$ is the wave vector, f is the wave frequency and n is the index of refraction for the medium. Because of the magnetic field, the plasma is anisotropic so that the value of n depends on the angle between $\underline{k}$ and the magnetic field $\underline{B}$ which is called the wave normal angle ψ as well as on the magnitude of B, the plasma density N and the effective ion mass Mi. Figure 2 illustrates the solution to the dispersion relation for a particular set of plasma parameters B, N and Mi, and for two wave normal directions $\psi = 0^o$ and $\psi = 90^o$. For some frequency ranges there can be two solutions which implies that several modes can co-exist with different characteristics. Waves with $\psi \sim 0^o$ have a polarization which is nearly circular--left-hand (L) or right-hand (R); waves with $\psi \sim 90^o$ tend to have a linear polarization (O-ordinary or X-extraordinary) and to have the power concentrated in the electric field or to be purely electrostatic. Associated with this diagram are many of the wave types identified in Figure 1 and Table I.

The index of refraction n depends on spatial location because the plasma parameters vary with spatial location. Figure 3 provides a model variation characteristic of the polar ionosphere and magnetosphere. According to Stix (1962), n can be expressed in terms of the wave frequency f, the electron plasma frequency f_p, the electron gyrofrequency f_g, equivalent ion frequencies involving the ion mass and the lower and upper hybrid frequencies LHR and UHR. These frequencies

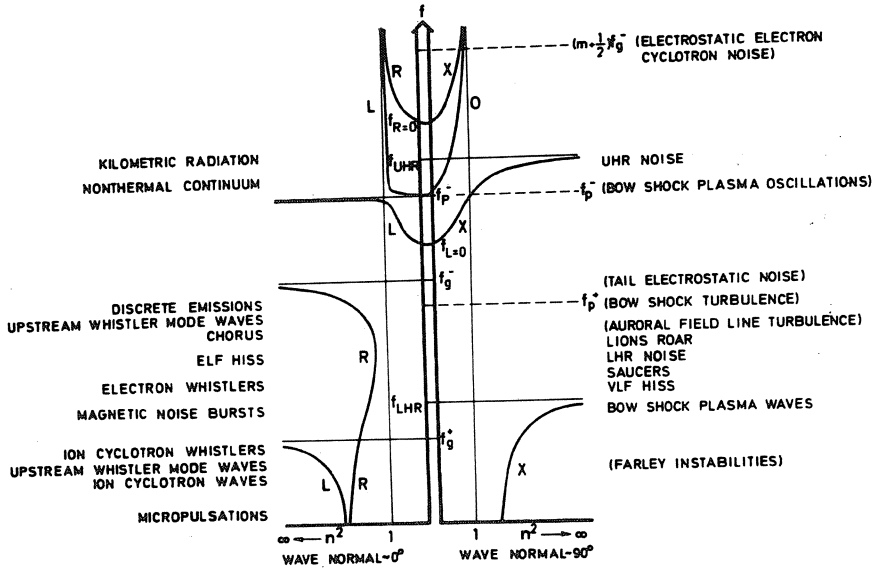

Figure 2. Association of plasma wave types with the characteristic frequencies of a plasma for wave normal directions nearly along the geomagnetic field direction (0^{o}) and nearly transverse (90^{o}). The curves represent the index of refraction, n, for the left-and right-hand (L and R) and the extraordinary and ordinary (X and O) wave modes. Waves in parentheses () are electrostatic. (Shawhan, 1979b).

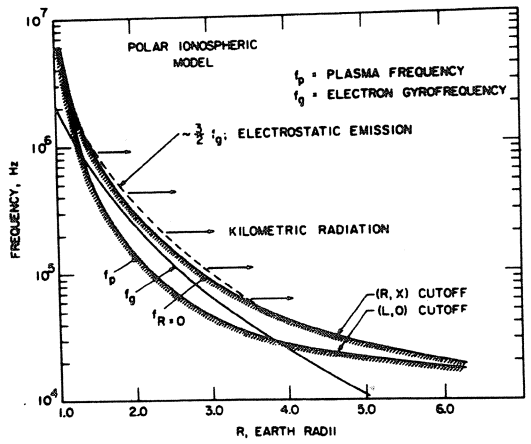

Figure 3. A model of the polar magnetosphere showing the variation of three characteristic plasmas frequencies with altitude--the electron gyrofrequency f_g, the electron plasma frequency f_p, and the right-hand mode cut-off F ($R=0$). (Gurnett, 1974)

are given as follows:

$$f_p = 9\times10^3\ N^{1/2}$$

$$f_g = 2.8\times10^6\ B$$

$$f(LHR)=(M_i/M_e)(1/f_p^2+1/f_g^2)^{-1/2} \qquad (2)$$

$$f(UHR)=(f_p^2+f_g^2)^{1/2}$$

where N is electrons/cm^3, B is in Gauss, and f in Hertz.

Current plasma wave research concentrates on understanding the various source mechanisms for the menagerie of plasma waves through theory, modelling and simulations. Both man-made and lightning discharge sources are remote from the magnetosphere and are reasonably well understood. The energy for plasma waves generated internal to the magnetosphere comes from the solar wind flow past the magnetosphere through electric fields and particle kinetic energy. Through plasma instabilities, a fraction of the free energy can be converted to a number of wave modes. Energy conversion mechanisms fall into two broad categories--gyroresonance and streaming instabilities. Gyroresonance is involved in the generation of chorus and the precipitation of trapped electrons by power line radiation. Streaming instabilities have a variety of forms--current driven, beam, two stream and drift wave, for example--which are responsible for most of the natural plasma waves. Some review papers on these mechanisms include Gendrin (1975), Anderson (1983) and papers in this volume--Scarf (1985), Ronnmark (1985), Matsumoto (1985), Gendrin (1985) and Fraser (1985).

3. WAVE RECEIVER SYSTEMS AND AMPLITUDE-FREQUENCY-TIME SPECTROGRAMS

The Dynamics Explorer-1 (DE) Plasma Wave Instrument is chosen to be representative of the many plasma wave antenna and receiver systems that have been flown throughout geospace, and the solar system. A detailed description of this system is given by Shawhan, et al (1981); more general discussions of system capabilities are given elsewhere (for example, Shawhan, 1970; S-300 Experimenters, 1978; and Shawhan, 1983). The DE-1 Spacecraft is depicted in the foreground of Figure 4. It exhibits two 6 meter booms; one with a magnetometer and the other with a short electric dipole antenna (ES), a searchcoil magnetic wave field antenna (H) and a 1 m^2 magnetic loop antenna (B). Two electric dipole antennas extend from the body itself--a 200 meter tip-tip wire electric antenna (EX) and a 9 meter tip-tip tubular electric antenna (EZ).

These five antenna systems are identified in the block diagram in Figure 5 along the five receiving systems that process the received electric and magnetic signals. Both the EX and the ES electric antennas are used for sensing the quasi-static electric field from DC-10Hz. The Step Frequency Correlation provides amplitude-frequency-time spectrograms of two wave components simultaneously and a cross-correlation spectrogram, every 32 seconds for 128 frequency steps between 100Hz and 400kHz. The Low Frequency Correlator extends the frequency range downward to 1.78Hz in 8 frequency steps. Examples of the composite

receiver electric field amplitude spectrogram outputs are displayed in Figures 6 and 7 from DE, and Figure 8 from ISEE-1. These receiver systems cover a wide frequency range but with frequency and/or time resolution compromised. Both the Linear Wideband Receiver and the Wideband Receiver in Figure 5 provide very high frequency and time resolution through ground processing but for a restricted frequency range. An example of the ISEE-1 Wideband Receiver output for auroral kilometric radiation is displayed in Figure 9.

In the DE-1 amplitude spectrograms of Figures 6 and 7, five orders of magnitude in frequency are displayed for a two hour time period with a 100dB amplitude range compressed into the gray-scale. This sort of display provides the basis for identifying the different species of waves in the menagerie and their dependence on the spatial position of the satellite. Note for example that auroral hiss has a characteristic "funnel shape" appearance, that AKR occurs only above the gyrofrequency, that Z-mode radiation occurs only when the plasma frequency f_p is below the gyrofrequency and that VLF transmitter signals cannot propagate for frequencies above the gyrofrequency. In the equatorial region of Figure 8, there are electrostatic emissions between harmonics of the gyrofrequency. With the poor time resolution of Figures 6 and 7, the AKR appears to be a continuous emission in frequency and time; in Figure 9, however, AKR is seen to be a super-position of narrow band, short-lived, rising and falling tones.

4. RAY TRACING ANALYSIS

Amplitude spectrograms provide information on the existence and the amplitude of plasma waves at the observing point. Waves may exist at that point either because they are generated in that region or because they are propagating through that region. It is essential to know the source region location in order to carry out measurements of the source plasma and to calculate growth rates for particular instability mechanisms. Ray tracing is a technique (as in optics) whereby the path of energy flow can be uniquely determined between the source and observer. In the magnetosphere the medium is inhomogeneous, anisotropic and supportive of more than one mode. In this volume, Kimura (1985) presents the basis for the technique and results for the Earth and other planets.

Ray tracing equations have been formulated by Haselgrove (1985). For two dimensions

$$\frac{dr}{dt} = \frac{1}{n^2}\left(P_r - n\frac{\partial n}{\partial P_r}\right)$$

$$\frac{d\theta}{dt} = \frac{1}{rn^2}\left(P_\theta - n\frac{\partial n}{\partial P_\theta}\right)$$

$$\frac{dP_r}{dt} = \frac{1}{n}\frac{\partial n}{\partial r} + P_\theta\frac{d\theta}{dt}$$

$$\frac{dP_\theta}{dt} = \frac{1}{r}\left(\frac{1}{n}\frac{\partial n}{\partial \theta} - P_\theta\frac{dr}{dt}\right)$$

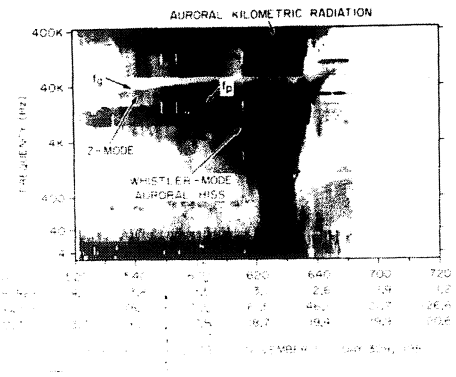

Figure 6. DE auroral zone pass with plasma frequency f_p much lower than gyrofrequency f_g. Note z-mode radiation. (Gurnett, et al, 1983)

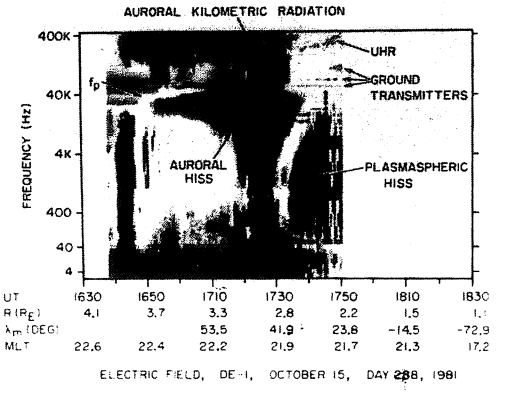

Figure 7. DE auroral zone pass with plasma frequency f_p greater than gyrofrequency f_g. Note UHR noise and VLF transmitters. (Gurnett, et al, 1983)

where r and θ are the radial distance and colatitude, n is the index of refraction, P_r and P_θ are the wave normal vector components with the magnitude of $\underline{n}$ and where t is the phase time along the ray path. These basic equations are also given for three dimensions which includes longitude and can be supplemented with equations for path length, group delay time and total growth or damping.

All the information about the plasma medium is contained in the expressions for the index of refraction which varies with spatial location (see Figure 3 for radial variation of parameters) and wave normal angle. Ray tracing programs consist of subroutines which contain at least analytical expressions for the plasma density N, the magnetic vector $\underline{B}$ and the ion composition and derivatives as a function of the spatial coordinates r, θ and longitude. The plasma dispersion expression n (f, $\underline{k}$) and various derivatives, and a solver routine for coupled partial differential equations. In practice many rays for different frequencies are started from the assumed source region and selected for analysis if they pass through the observation point. Results from a ray tracing analysis to understand the "funnel-shaped" auroral hiss in Figure 7 are presented in Figures 10 and 11 (Gurnett,et al, 1983). Figure 10 shows ray paths for different frequencies on auroral field lines for one source altitude. Figure 11 indicates that the best match to the observations occurs for a source at 1.7 to 1.9R_E. Impressive results for different modes of auroral kilometric radiation are given by Hashimoto (1984) and for AKR path growth by Omidi and Gurnett (1984), as other examples.

5. WAVE VECTOR AND WAVE DISTRIBUTION FUNCTION ANALYSIS

More information is needed and available from the wave fields than just amplitudes to characterize the waves as to nature--electrostatic or electromagnetic, to polarization--circular or linear, to direction of propagation and to the wave normal direction--$\underline{k}$. This information is needed to determine the wave mode, the probable source location since $\underline{k}$ is needed for ray tracing and wave-particle interaction mechanisms. A review of wave vector analysis is given by Shawhan (1983). Through the use of multiple antennas and receivers and cross-correlation of the waveforms these additional quantities can be obtained. A summary of some measurements to date are as follows:

FR-1	1964	Wave Normal Vector
Injun-5	1969	VLF Up/Down Direction
Voyager	1977	HF Wave Polarization
ISEE	1978	VLF Wave Normal and Up/Down Direction
GEOS	1979	ULF/ELF/VLF Wave Normal Vector
DE	1981	ELF/VLF Polarization and Up/Down Direction

Results from the DE-1 polarization measurement are shown in Figure 12 which gives the satellite-source geometry and in Figure 13 which gives an amplitude spectrogram and a polarization spectrogram. By correlating the long electric antenna EX when it is rotated perpendicular to the probable auroral zone source direction and EX which is perpendicular to the orbit plane, the polarization Right-hand (black) or Left-hand (white) can be obtained at each frequency step (Mellott, et al, 1984). Auroral hiss is known to be in the whistler mode or Right-hand mode in this kHz frequency range. Figure 13 illustrates that the strong AKR is also Right-hand but there is a weaker Left-hand component observable over a larger spatial extent which is consistent with the ray tracing analysis of Hashimoto (1984).

In reality the wave source regions are extensive in size and there exists many paths between the source region and the observing point. Consequently, there is not a unique $\underline{k}$-vector for a source but rather a distribution of $\underline{k}$-vectors. Lefeuvre and his co-workers have developed theoretical and computational techniques to derive this wave distribution function WDF from the available wave field information. At most there are six electromagnetic wave components--three electric and three magnetic. All autocorrelation and cross-correlation products provide 36 quantatives with which to estimate the WDF. In practice models of the WDF with adjustable parameters are fit to the correlation data to obtain a best-fit solution. Some sample results are presented in Figure 14 (Lefeuvre, et al, 1982). For this case the WDF is fairly well concentrated at a given direction. In other cases multiple sources are found. The output of these WDF analyses can provide the input for more realistic ray tracing analyses.

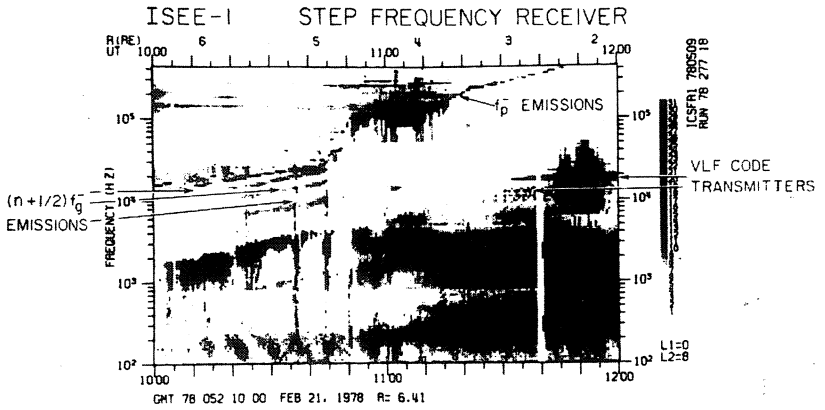

Figure 8. Spectrogram of emissions in the equatorial region from 2 to 6.5 earth radii from the International Sun-Earth Explorer (ISEE). Emission near the electron plasma frequency f_p called non-thermal continuum radiation are observed as are electrostatic emissions between harmonics of the electron gyrofrequency $(n+1/2)f_g$. (Shawhan, 1979b)

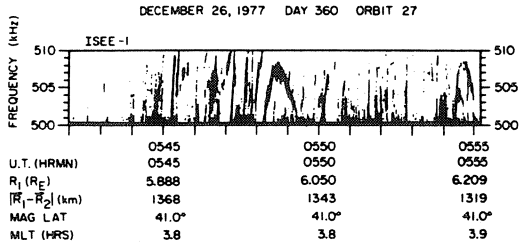

Figure 9. High time frequency resolution display of auroral kilometric radiation from the ISEE-1 wideband receiver. Signals are in the range of 500 to 510 kHz with 13 minutes of data displayed. The AKR is made up of many narrow band rising and falling tones. (Gurnett, et al, 1979)

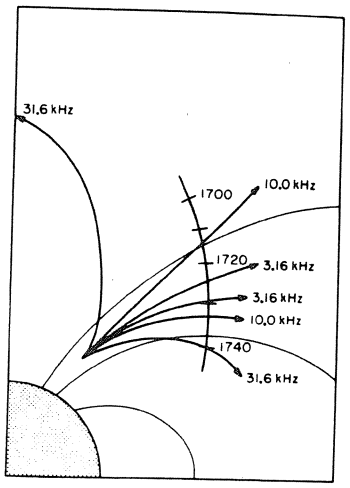

Figure 10. Ray paths computed for different frequencies from a source position on auroral field lines. (Gurnett, et al, 1983)

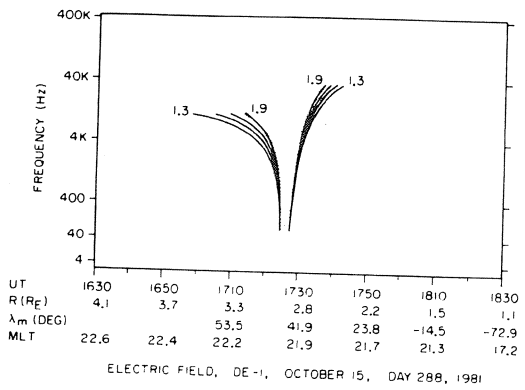

Figure 11. Frequency-time plots for the ray paths in Figure 11 for source positions located in the range of 1.3 to 2.1 Earth radii. Note that source positions of 1.7 to 1.9 R_E give the best fit to this funnel-shaped auroral hiss event shown on the spectogram in Figure 7. (Gurnett, et al, 1983)

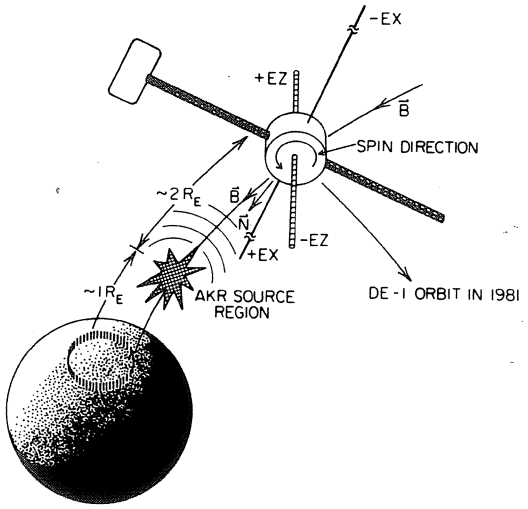

Figure 12. Geometry of the DE-1 spacecraft with respect to the auroral kilometric radiation source region.

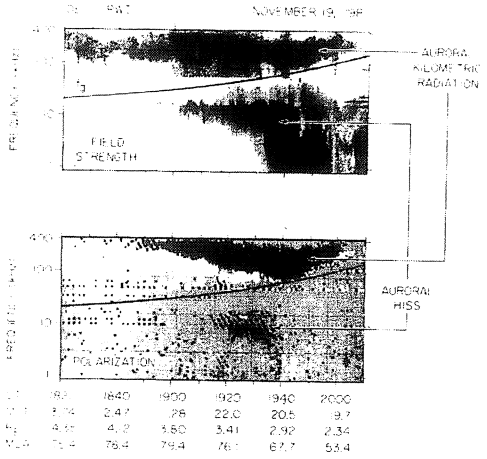

Figure 13. Frequency-time amplitude (top) and polarization (bottom) spectrograms of auroral kilometric radiation and auroral hiss as measured with DE-1. Electric field intensities are from the EX antenna and polarization is determined between EX and EZ (see Figure 12). Black indicates right-hand polarized waves and white, left-hand. The electron gyrofrequency is also plotted. Note that the intense AKR is right-hand polarized. (Mellott, et al, 1984)

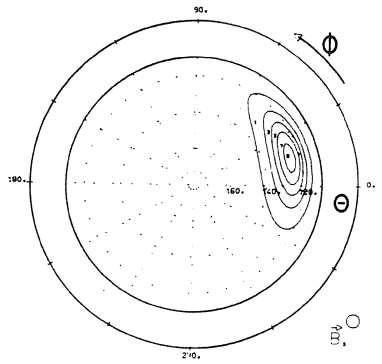

Figure 14. Wave Distribution Function (WDF) for a VLF transmitter signal received on GEOS derived from three wave magnetic components. (Lefeuvre, et al, 1982)

6. AREAS FOR FURTHER RESEARCH

Significant progress in plasma wave research to support the increasing efforts in theory, modelling and simulations could be achieved in the following areas:

- Develop waveform capture receivers so that samples of all six wave components can be analyzed for wave vector and WDF characteristics with high time and frequency resolution
- Enhance ray tracing analysis by improving the plasma parameter models and by carrying out growth rate calculations
- Improve WDF algorithms and apply the method to many more cases
- Carry out and analyze active wave propagation and wave-particle experiments under controlled conditions utilizing the Shuttle/Spacelab

7. REFERENCES

Al'pert, Ya. L., Waves and Satellites in the Near-Earth Plasma, Consultants Bureau: New York, 1974.

Anderson, R. R., Plasma Waves in Planetary Magnetospheres, Rev. Geophys. Space Phys., 21, 474-494, 1983.

Fraser, B. J., Observations of Ion Cyclotron Waves Near Geosynchronous Orbit and on the Ground, this volume, 1985.

Gendrin, R., Waves and Wave-Particle Interactions in the Magnetosphere; A Review, Space Sci. Rev., 18, 145-200, 1975.

Gendrin, R., Consequences of Hydromagnetic Waves on Magnetosphere Particle Dynamics, this volume, 1985.

Gurnett, D. A., The Earth as a Radio Source; Terrestrial Kilometric Radiation, J. Geophys. Res., 79, 4227-4238, 1974.

Gurnett, D. A., R. R. Anderson, F. L. Scarf, R. W. Fredricks and E. J. Smith, Initial Results from ISEE-1 and ISEE-2 Plasma Wave Investigation, Space Sci. Rev., 23, 103-777, 1979.

Gurnett, D. A., S. D. Shawhan and R. R. Shaw, Auroral Hiss, Z Mode Radiation, and Auroral Kilometric Radiation in the Polar Magnetosphere; DE-1 Observations, J. Geophys. Res., 88, 329-340, 1983.

Hasselgrove, J., Ray Theory and a New Method for Ray Tracing, London Physical Soc.: Report on Conf. Phys. Ionosphere, pp. 355-364, 1955.

Hashimoto, Kozo, A Reconcilliation of Propagation Modes of Auroral Kilometric Radiation, J. Geophys. Res., 89, 7459-7466, 1984.

Helliwell, R. A., Whistlers and Related Ionospheric Phenomena, Stanford University Press; Stanford, 1965.

Kimura, I., Whistler Mode Propagation in the Earth and Planetary Magnetospheres and Ray Tracing Technique, this volume, 1985.

Lefeuvre, F., T. Neubert and M. Parrot, Wave Normal Directions and Wave Distrbution Functions for Ground-Based Transmitter Signals Observed With GEOS-1, J. Geophys. Res., 87, 6203-6217, 1982

Matsumoto, H., Coherent Non-Linear Effects on Electromagnetic Wave-Particle Interactions and Relevant Diagnostics in Simulations, this volume, 1985.

Mellott, M. M., W. Calvert, R. L. Huff, D. A. Gurnett and S. D. Shawhan, DE-1 Observations of Ordinary Mode and Extraordinary Mode Auroral Kilometric Radiation, Geophys. Res. Lett., 11, 1188-1191, 1984.

Omidi, N. and D. A. Gurnett, Path-Integrated Growth of Auroral Kilometric Radiation, J. Geophys. Res., 89, 10801-10812, 1984.

Ronnmark, K., Kinetic Theory of Plasma Waves, this volume, 1985.

S-300 Experimenters, Introduction to the S-300 Experiments Onboard GEOS; Space Sci. Rev., 22,327-332, 1978.

Scarf, F. L., Wave Observations in Outer Planet Magnetospheres, this volume, 1985.

Shawhan, S. D., The Use of Multiple Receivers to Measure the Wave Characteristics of Very-Low-Frequency Noise in Space, Space Sci. Rev., 10, 689-736, 1970.

Shawhan, S. D., Magnetospheric Plasma Waves, Solar System Plasma Physics, C. F. Kennell, L. J. Lanzerotti and E. N. Parker, (eds.), Volume III, 211-270, North-Holland; Amsterdam, 1979a.

Shawhan, S. D., Magnetospheric Plasma Wave Research 1975-1978, Rev. Geophys. Space Phys., 17, 705-724, 1979b.

Shawhan, S. D., Estimation of Wave Vector Characteristics, Adv. Sci Res., 2, 31-41, 1983.

Shawhan, S. D., D. A. Gurnett, D. L. Odem, R. A. Helliwell and C. G. Park, The Plasma Wave and Quasi-Static Electric Field Instrument (PWI) for Dynamics Explorer-A, Space Sci. Instrumentation, 5, 535-550, 1981.

Stix, T. H., Theory of Plasma Waves, McGraw Hill: New York, 1962.